COMPDYN 2015
5th ECCOMAS Thematic Conference on
Computational Methods in Structural Dynamics and Earthquake Engineering
M. Papadrakakis, V. Papadopoulos, V. Plevris (eds.)
Crete Island, Greece, 25–27 May 2015

OPTIMAL DESIGN AND DYNAMICS OF TRUSS BRIDGES

G. Carpentieri[1], M. Modano[2], F. Fabbrocino[3] and F. Fraternali[1]

[1]Department of Civil Engineering , University of Salerno
Via Giovanni Paolo II, 132, 84084, Fisciano (SA), Italy
e-mail: gcarpentieri@unisa.it (G. Carpentieri), f.fraternali@unisa.it (F. Fraternali)

[2] Department of Structural Engineering, University of Naples
80132, Naples (NA), Italy
e-mail: modano@unina.it (M. Modano)

[3] Department of Engineering, Pegaso Telematic University
80132, Naples (NA), Italy
e-mail: frfabbro@unina.it (F. Fabbrocino)

Keywords: Truss structures, Tensegrity, form-finding, minimum mass, optimal complexity, prestress, vibration modes.

Abstract. *Bridge structures have attracted the interest of Engineers throughout the history because they represent the attempt of men to overcome obstacles. Bridges allow easier connections between two different points and faster displacements of goods and people. The present work makes use of truss structures to search for the most efficient bridges. We first present numerical results for minimal mass truss bridge designs. Our approach creates a network of tensile and compressive members distributed throughout the system at many different scales. We leave the prestress calibration to a second step of our design strategy, to be carried out after the minimal mass topology has been determined, with the aim of optimizing the dynamic performance of the structure. A numerical example shows that the vibration modes of the examined bridge model can be tuned by playing with the prestress of the deck members.*

1 INTRODUCTION

Tensegrity structures are axially loaded prestressable structures. Motivated by nature, where tensegrity concepts appear in every cell, in the molecular structure of the spider fiber, and in the arrangement of bones and tendons for control of locomotion in animals and humans, Engineers have only recently developed efficient analytical methods to exploit tensegrity concepts in engineering design. Previous attempts to judge the suitability of tensegrity for engineering purposes have simply evaluated the tensegrity produced as art-forms, but then judges them according to a different (engineering) criteria. The development of "tensegrity engineering" should allow tensegrity concepts to be optimized for the particular engineering problem at hand, rather than simply evaluating a structure designed only for artistic objectives. The development of such tensegrity engineering methods is the continuing goal of our research.

The tensegrity paradigm used for bridges in this paper allows the marriage of composite structures within the design. Our tensegrity approach creates a network of tension and compressive members distributed throughout the system at many different scales (using tensegrity fractals generates many different scales). Furthermore, these tension and compression members can simultaneously serve multiple functions, as load-carrying members of the structure, and as sensing and actuating functions. Moreover, the choice of materials for each member of the network can form a system with special electrical properties, special acoustic properties, special mechanical properties (stiffness, etc). The mathematical tools of this paper can be used therefore to design metamaterials and structural networks (cf., e.g., [1–9]) with unusual and very special properties not available with normal design methods.

This paper focuses on bridge design for minimal mass. The subject of form-finding of tensegrity structures continues to be an active research area [10–15], due to the special ability of such structures to serve as controllable systems (geometry, size, topology and prestress control), and also because the tensegrity architecture provides minimum mass structures for a variety of loading conditions, [16–19]. Particularly interesting is the use of fractal geometry as a form-finding method for tensegrity structures, which is well described in [16–18, 20]. Such an optimization strategy exploits the use of fractal geometry to design tensegrity structures, through a finite or infinite number of self-similar subdivisions of basic modules. The strategy looks for the optimal number of self-similar iterations to achieve minimal mass or other design criteria. This number is called the optimal *complexity*, since this number fixes the total number of parts in the structure.

The self-similar tensegrity design presented in [16–18] is primarily focused on the generation of *minimum mass* structures, which are of great technical relevance when dealing with tensegrity bridge structures (refer, e.g., to [21]). The 'fractal' approach to tensegrity form-finding paves the way to an effective implementation of the tensegrity paradigm in *parametric architectural design* [11, 12, 22, 23].

Designing tensegrity for engineering objectives has produced minimal mass solutions for five fundamental (but planar) problems in engineering mechanics. Minimal mass for tensile structures, (subject to a stiffness constraint) was motivated by the molecular structure of spider fiber, and may be found in [24]. Minimal mass for compressive loads may be found in [16]. Minimal mass for cantilevered bending loads may be found in [17]. Minimal mass for torsional loads may be found in [18]. Discussions of minimal mass solutions for distributed loads on simply-supported spans, where significant structure is not allowed below the roadway, may be found in [25]. It is also worth noting that tensegrity structures can serve multiple functions. While a cable is a load-carrying member of the structure, it might also serve as a sensor or

actuator to measure or modify tension or length. Other advantages of tensegrity structures are related to the possibility to integrate control functions within the design of the structure. A grand design challenge in tensegrity engineering is to coordinate the structure and control designs to minimize the control energy and produce a structure of minimal mass. This would save resources (energy and mass) in two disciplines, and therefore "integrate" the disciplines [26].

This paper reviews the minimum mass design of tensegrity structures carrying distributed bending loads (Sects. 2, 3), which has been diffusely presented in [25], and investigates on the vibration modes of the examined bridge model by varying the state of prestress applied to the structure (Sect. 4). Prestress design is a typical feature of tensegrity systems. The procedure illustrated in [25] returns the minimal mass structure, for a given loading condition, together with a certain prestress state. By changing such a prestress, while increasing the mass, one can improve the ability of a structure to tolerate larger uncertainties in the external loading, and avoid slackening problems in cables. We leave the prestress calibration to a second step of our design strategy, to be carried out after the minimal mass topology has been determined, with the aim of optimizing the dynamic performance of the structure.

2 TENSEGRITY BRIDGE MODEL

In a famous work dated 1904, A.G.M. Michell examines the problem of finding the minimum volume network of fully stressed truss elements, which transmit a vertical force applied at the middle point C of a given segment AB to two fixed hinge supports applied at A and B [27]. On pages 594-597 of this work, Michell deals with a truss network spanning a 2D continuous domain including the points A, B and C along its boundary (*centrally loaded beam*), and assumes that the material of such a domain is homogenous. Without entering the mathematical aspects of Michell's problem (refer, e.g., to [28]), we notice that the Michell topology under consideration includes a portion DE of a circumference centered in C, the segments DA and EB lying on the tangents in D and F to the arch DE, and all the radii of the circular sector CDE (cf. Fig. 1, where the compressive elements (or *bars*) of the Michell frame are represented through thick black lines, while the tensile elements (or *strings*) are represented through thin red lines). Such a topology can be applied to both the regions placed above and below the applied force F, with the difference that the arch ADEB (hereafter also called Michell arch) works in compression and the radii pointing to C work in tension in the first case (Fig. 1, top), while, on the contrary, the arch ADEB works in tension and the radii pointing to C work in compression in the second case (Fig. 1, bottom). It is worth noting that the central angle of the circular sector CDE gets larger and larger, as the angle α (or β) gets closer and closer to 90 deg (Fig. 1).

We here introduce a parametric model of a tensegrity bridge obtained through n self-similar subdivisions of a basic module. This module is formed by a single Michell arch showing p radii, placed above the deck of the bridge, and two arches, each of them showing $q = p$ radii, placed below the deck. Such a bridge is constrained by a fixed hinge support at one end of the deck, and a rolling hinge support at the other end. We show the basic module corresponding to $n = p = 1$ in Fig. 2, while more complex shapes corresponding to higher values of n and p are shown in Fig. 3 of [25]. Notice how each arch above the deck features p radii, and each arch below the deck features q radii, with $p = q$. The angles α and β can assume arbitrary values, and the horizontal elements at the level of the deck (represented through blue lines in Fig. 2) can work either in tension or in compression (*bidirectional elements*, cf. [19]). Such elements provide the horizontal components of the lateral (supporting) forces of the Michell arch (Fig. 1). The basic module shown in Fig. 2 exhibits a single compressed arch above the deck, two

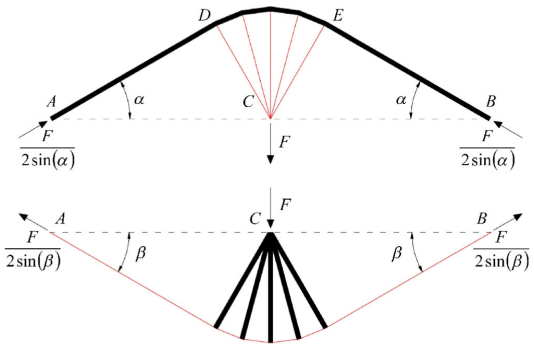

Figure 1: Michell frames for a centrally loaded beam.

tensile chords below the deck and a subdivision of the deck into four elements of equal length. Hereafter, we let f denote the total force transferred from the deck to the bridge structure. For $n > 1$, we assume that the elements of the nested arches placed above the deck can overlap each other. Moreover, to consider a common requirement for bridges over navigable water, we discard the outer arches placed below the deck (indicated by dotted lines in Fig. 3 of [25]), in order to reduce the size of the substructure below the deck, for clearance above the water. In a real bridge structure, the elements placed above the deck would have a 3D geometry that prevents member overlapping. It is worth noting that the geometry corresponding to an arbitrary number n of self-similar subdivisions of the basic module features 2^{n+1} elements at the level of the deck, and show nodal forces equal to $f/(2^{n+1})$ in correspondence with the intermediate nodes placed at the level of the deck. The following variables completely define the geometry of the bridge structure: the total span L, the 'top aspect angle' α, the 'bottom aspect angle' β, and the complexity parameters n, p and q. The total numbers of top arches, n_{ta}, bottom arches, n_{ba}, strings, n_s, bars, n_b, and nodes, n_n, are given by:

$$n_{ta} = 2^n - 1, \quad n_{ba} = 2^n, \tag{1}$$

$$n_s = q n_{ta} + (p+1)\, n_{ba} + 2^{n+1}, \quad n_b = (q+1)\, n_{ta} + p n_{ba} + 2^{n+1}, \tag{2}$$

$$n_n \;=\; q\; n_{ta} + p\; n_{ba} + 2^{n+1} + 1. \tag{3}$$

As to the node coordinates, we observe that the nodes belonging to the 'superstructure' (i.e., the portion of the bridge placed above the deck) lie on n nested circumferences with radii R_{t_i} $(i = 1, ..., n)$, while the nodes of the 'substructure' instead lie on sequential circumferences with radius R_b. Such radii are computed as follows

$$R_{t_i} = \frac{L}{2^i} \sin\alpha, \;\; (i = 1, ..., n); \quad R_b = \frac{L}{2^n} \sin\beta. \tag{4}$$

We look for the optimal values of the complexity parameters n, p and q and the aspect angles α and β, which minimize the mass of the bridge under yielding and buckling constraints. As anticipated, we prescribe $q = p$ and we assume that all bars and strings are made up of the same material, for the sake of simplicity. The removal of such constraints is not a big issue from the theoretical point of view, but might lead to a significant increase in the number of optimization variables.

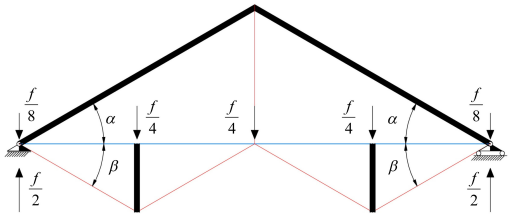

Figure 2: Basic module of the tensegrity bridge ($n = 1$, $p = 1$).

3 MINIMAL MASS DESIGN

In this section we present a collection of numerical results extracted from [25], which aim to illustrate the potential of the minimum mass design under consideration. We use the symbols μ^*, α^* and β^* to denote the minimum mass and the optimal aspect angles of the tensegrity bridge under combined yielding and buckling constraints, respectively, and the symbols μ_Y^*, α_Y^* and β_Y^* to denote the optimal values of the same quantities under simple yielding constraints. In all the examples, we search for a global minimum mass configuration of the bridge, by recursively running the optimization procedure presented in [25], so that the design variables n, p, α and β may range within prescribed search domains. We set the step increments of n and p to 1, the step increments of α and β to 0.01 deg. In addition, we set L, f and ρ to unity, in abstract units, and make use of the following assumptions: $\bar{\sigma}_Y = 6.9 \times 10^8 L^2/f$; $E = 2.1 \times 10^{11} L^2/f$. In order to highlight the relative 'weight' of the elements placed at the level of the deck, we introduce the following ratios,

$$\frac{\mu_{db}^*}{\mu_b^*}, \quad \frac{\mu_{ds}^*}{\mu_s^*}. \tag{5}$$

where μ_{db}^*, μ_{sb}^*, μ_b^*, μ_s^* denote the total mass of the bars placed at the level of the deck, the total mass of the strings placed at the level of the deck, the overall mass of the bars and the overall mass of the strings, respectively, in correspondence with any arbitrary minimum mass configuration under combined yielding and buckling constraints. We remind the reader that the elements placed at the level of the deck are bidirectional, in the sense that they can contemporarily serve as bars or strings [19].

The examined minimum mass design assumes that all the design variables n, p, α, and β may simultaneously vary within the following bounds,

$$n \in [1, 5], \quad p \in [1, 7], \quad \alpha \in (0, 90) \text{ deg}, \quad \beta \in (0, 90) \text{ deg}. \tag{6}$$

The most relevant results corresponding to the present case are illustrated in Tab. 1 and Fig. 3. The results in Tab. 1 highlight that the global minimum mass configuration under combined yielding and buckling constraints is reached for $n = 2$, $p = 7$ ($\mu^* = 333.17$, $\alpha^* = 62.52$ deg, $\beta^* = 17.77$ deg), within the search domain (6). Referring to the case with $n = 2$, in order to detect if the global minimum mass configuration is obtained for finite complexity p or not, we let this parameter grow up to $p = 13$, and determine the corresponding relative minimum mass configurations of the bridge. We find out that the mass of the bridge monotonically decreases when p grows from 1 to 13, and n remains equal to 2. In particular, the relative minimum mass configuration for $n = 2$ and $p = 13$ is the following: $\mu^* = 225.98$, $\alpha^* = 69.45$ deg, $\beta^* = 23.97$ deg. Such results, together with those presented in Tab. 1, indicate that the global minimum mass configuration of the bridge might be achieved either for rather large values of p, or in the limit $p \to \infty$, when $n \geq 2$.

n	p	α_Y^*	β_Y^*	μ_Y^*	α^*	β^*	μ^*
1	1	41.83	24.11	1.1180	26.11	13.77	808.84
1	11	54.44	34.97	0.9867	53.42	33.97	337.69
1	20	54.65	35.18	0.9855	51.98	32.60	352.24
2	1	44.62	9.34	1.5207	26.58	4.77	1086.23
2	3	57.81	14.83	1.3329	45.20	9.53	558.02
2	7	66.42	20.90	1.2534	62.52	17.77	333.17
3	1	44.96	4.08	1.7545	26.58	2.05	1186.33
3	3	59.52	6.92	1.5232	45.31	4.13	607.67
3	7	72.52	12.78	1.4137	63.71	8.23	354.03
4	1	44.96	1.91	1.8761	26.58	1.03	1221.82
4	3	59.73	3.27	1.6256	45.31	1.93	625.75
4	7	75.51	7.35	1.5021	63.82	3.88	363.95
5	1	45.01	0.93	1.9378	26.58	0.75	1234.39
5	3	59.92	1.60	1.6784	45.32	1.44	632.19
5	7	76.80	3.96	1.5489	63.83	1.88	367.65

Table 1: Selected results for the minimal mass design of the examined bridge model.

By adding gravity forces [19], and referring to the case with $n = 2$ and $p = 13$, we obtain $\mu^* = 227.49$, $\alpha^* = 69.48$ deg, and $\beta^* = 23.52$ deg. Such results show that the inclusion of self-weight does not cause a significant change of the minimum mass configuration at hand. As to the elements placed at the level of the deck, we observe the following results: $\mu^*_{db}/\mu^*_b \ll 1$, and $\mu^*_{ds}/\mu^*_s \ll 1$, for $n \leq 3$. The ratio μ^*_{ds}/μ^*_s becomes relevant for $n > 3$, being equal to 0.06 for $n = 4$ and $p = 1$, and 0.3 for $n = 5$ and $p = 1$. Nevertheless, the same ratio decreases with p for fixed n, being equal to $\approx 10^{-4}$ for $n = 4$ and $p = 7$, and $\approx 10^{-5}$ for $n = 5$ and $p = 7$. We can therefore conclude that such elements serve as tensile members (strings) for $n > 1$, and that their structural relevance increases with n and decreases with p. It is also seen from Tab. 1 that, in each of the examined cases, the optimal values of α very slowly increase with n, and rather markedly increase with p. The optimal values of β instead markedly decrease with n, and significantly increase with p. It is worth noting that the two examined design strategies (simple yielding constraints and combined yielding and buckling constraints) lead to rather different aspect ratios of the bridge for $p = 1$, and, on the contrary, to more similar geometries as p gets larger, for any given n (cf. Tab. 1). The results shown in Fig. 3 emphasize that the current minimum mass design of the bridge leads to rather large values of α and considerably small values of β, as the complexity parameters n and p progressively increase. In particular, the bottom height of the bridge dramatical shrinks for $n \geq 3$ (Fig. 3). This is explained by observing that the lower chords of the bridge carry tensile forces $t_{ba} = \frac{f_n}{2Sin(\beta)}$ (cf. Fig. 1), with $f_n = f/(2^{n+1})$. As n goes to infinity and β goes to zero, it can be verified that t_{ba} approaches a finite limit. The solution with $\beta \to 0$ becomes convenient in terms of mass savings as $n \to \infty$, since it reduces the lengths of the tensile chords and compressed rays placed below the deck. We wish to remark, however, that the global minimum mass configuration is achieved for $n = 1$ under simple yielding constraints, and $n = 2$ under combined yielding and buckling constraints.

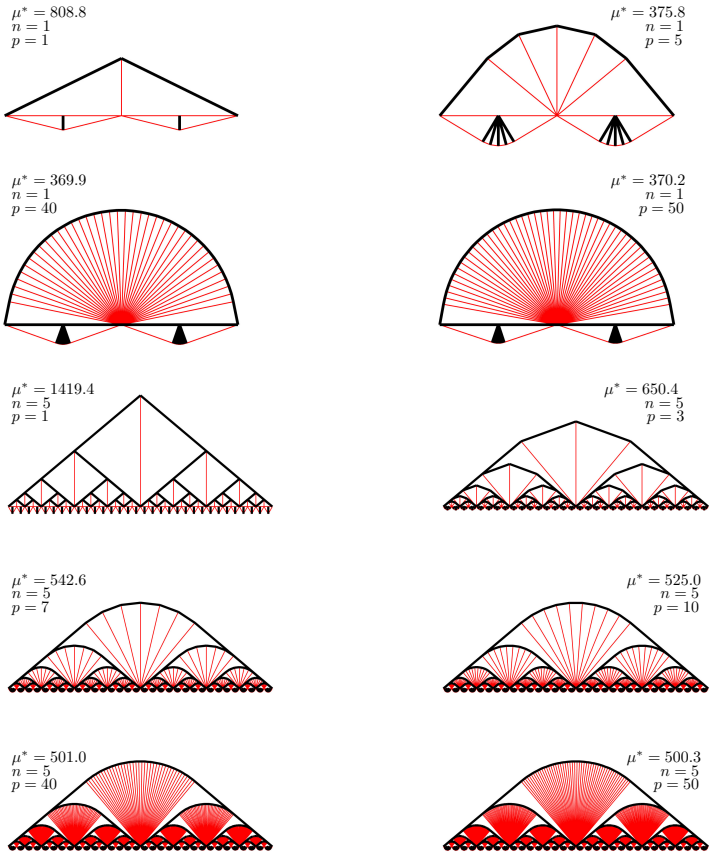

Figure 3: Optimal topologies under combined yielding and buckling constraints for different values of the examined design variables.

4 VIBRATION MODES

It is worth noting that the minimal mass design illustrated in the previous section leads to statically determinate structures with no applied prestress. Nevertheless, the prestress design is of great importance for a number of properties of tensegrity structures, including structural stiffness, stability and dynamics (refer, e.g., to [10–15, 29] and references therein). In particular, an optimal prestress design oriented to control the free vibration modes and frequencies of the structure awaits attention, being at present only partially investigated in the literature [29].

We study the influence of the prestress design on the dynamical response of the present bridge model with reference to the the basic module in Fig. 2, assuming optimal aspect angles ($\alpha = 26.11\ deg$, $\beta = 13.77\ deg$). In order to allow statically indeterminacy, which is necessary to permit the existence of self equilibrated member forces, we replace the roller hinge support of such a structure with a fixed hinge. As a consequence, we allow the string elements placed at the level of the deck to be axially prestrained of an arbitrary quantity p (*deck prestrain*). The assumed material is steel for all members (Young modulus $E = 210\ GPa$, yield strength $\sigma_y = 690\ MPa$); the total span of the bridge is set equal to $30\ m$; and the total bridge weight (including the deck) is set equal to $450\ kN$.

Fig. 4 shows the first vibration modes of the basic module under zero deck prestress ($p = 0$), and deck prestress corresponding to $p = 10^{-3}$. We observe that the vibration mode of the prestressed structure is slightly different from that of the structure under zero prestress. As a matter of fact, the first vibration mode of the structure for $p = 10^{-3}$ features a ratio $\eta = 7.5$ between the vertical displacement at the central node of the deck and the vertical displacements

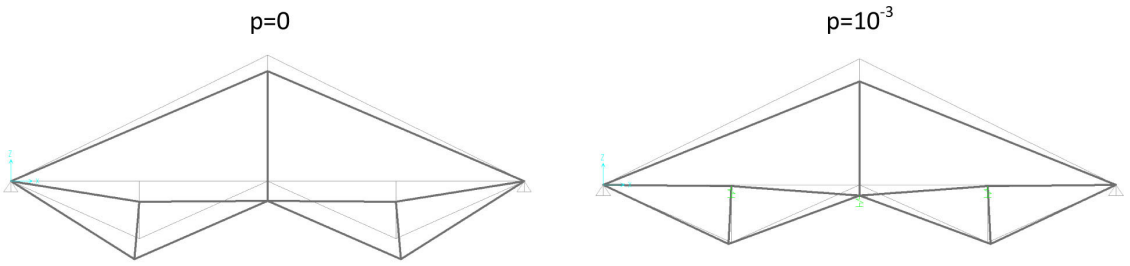

Figure 4: First vibration mode for different prestrains of deck members.

at the nodes of the deck placed at one quarter of the bridge span, i.e. prevalent vertical deflection at the midspan (cf. Fig. 4-right). The vibration mode of the structure under zero prestress instead exhibits $\eta = 0.96$ (cf. Fig. 4-left), i.e. vertical displacements at the lateral nodes of the deck that are comparable to that of the central node. It is also with noting that the structure under $p = 0$ exhibits first natural frequency which is 3.5% lower than the first natural frequency of the structure undergoing $p = 10^{-3}$.

5 CONCLUDING REMARKS

A first goal of the present study has been concerned with the minimal mass design of tensegrity bridge structures. The forces, locations, and number of members of a parametric bridge model in 2D have been optimized to minimize mass subject to both buckling and yielding constraints. We have optimized the complexity of the structure, where structural complexity as the number of members in the design. This can be related to 3 parameters (n, p, q), where 2^n is the number of deck sections along the span; p is the number of compressive members (bars) reaching from the span center to the *substructure*; and q is the number of cables reaching from the span center to the *superstructure*. Hence we refer to (n, p, q) as the three different kinds of *complexities* of the structure. We used a tensegrity structural paradigm which allowed these several kinds of complexities. The complexity n has been determined by a self-similar law to fill the space of the bridge. As the number of self-similar iterations goes to infinity we get a tensegrity fractal topology. The numerical results presented in Sect. 3 have pointed out that the global minimum mass configuration of the examined bridge model shows finite complexity n, and markedly large or infinite complexities $p = q$. We can therefore conclude that such a bridge feature a multiscale, discrete-continuum complexity. Concerning the aspect ratios of the bridge, we have observed that, as the complexity n increases, the height of the portion of the bridge placed above the deck increases, while the height of the structure placed below the deck decreases dramatically.

An illustrative example regarding the first vibration mode of the basic module ($n = p = q = 1$) has demonstrated that the application of a state of prestress to the string elements placed at the deck level may significantly affect the geometry of such a mode and the associated natural frequency. A comprehensive study on the dynamics of tensegrity bridges will follow as future work, to impose suitable design constraints on stiffness issues (vibrational frequencies, mode shapes, displacements for high winds conditions, etc). It is worth noting, however, that the capability all of these choices and adjustments are within the free parameters of the designs in this work. The subsequent dynamics approach will evaluate the value (economics and performance tradeoffs) the use of feedback control for the deployable and service functions, or to adjust the stiffness of the structure (varying the prestress of the cables) to modify stiffness or damping after storm damage.

References

[1] C. Daraio, D. Ngo, V.F. Nesterenko, F. Fraternali, Highly nonlinear pulse splitting and recombination in a two-dimensional granular network. *Physical Review E*, 82:036603, 2010.

[2] D. Ngo, F. Fraternali, C. Daraio, Highly nonlinear solitary wave propagation in Y-shaped granular crystals with variable branch angles. *Physical Review E*, 85:036602, 2012.

[3] F. Fraternali, C.D Lorenz, G. Marcelli, On the estimation of the curvatures and bending rigidity of membrane networks via a local maximum-entropy approach. *Journal of Computational Physics*, **231**, 528-540, 2012.

[4] B. Schmidt, F. Fraternali, Universal formulae for the limiting elastic energy of membrane networks. *Journal of the Mechanics and Physics of Solids*, **60**, 172-180, 2012.

[5] F. Fraternali, L. Senatore, C. Daraio, Solitary waves on tensegrity lattices. *Journal of the Mechanics and Physics of Solids*, **60**, 1137-1144, 2012.

[6] F. Fraternali, I. Farina, G. Carpentieri. A discrete-to-continuum approach to the curvatures of membrane networks and parametric surfaces. *Mechanics Research Communications*, **56**, 18-15, 2014.

[7] A. Amendola, F. Fraternali, G. Carpentieri, M. de Oliveira, R. E. Skelton, Experimental investigation of the softening-hardening response of tensegrity prisms under compressive loading. *Composite Structures*, **117**, 234-243, 2014.

[8] F. Fraternali, G. Carpentieri, A. Amendola, On the mechanical modeling of the extreme softening/hardening response of axially loaded tensegrity prisms. *Journal of the Mechanics and Physics of Solids*,**74**, 136-157, 2015.

[9] F. Fraternali, G. Carpentieri, A. Amendola, R. E. Skelton, V. F. Nesterenko, Multiscale tunability of solitary wave dynamics in tensegrity metamaterials. *Applied Physics Letters*, **105**, 201903, 2014.

[10] K. Koohestani, Form-finding of tensegrity structures via genetic algorithm. *International Journal of Solids and Structures*, 49,739–747, 2012.

[11] L. Rhode-Barbarigos, H. Jain, P. Kripakaran, I.F.C. Smith, Design of tensegrity structures using parametric analysis and stochastic search. *Engineering with Computers*, 26(2),193–203, 2010.

[12] T. Sakamoto , A. Ferrè, M. Kubo, (Eds.), *From Control to Design: Parametric/Algorithmic Architecture*, Actar, 2008.

[13] T. Sokóf, G.I.N. Rozvany, New analytical benchmarks for topology optimization and their implications. Part I: bi-symmetric trusses with two point loads between supports. *Structural and Multidisciplinary Optimization*, 46,477–486, 2012.

[14] A.G. Tilbert, S. Pellegrino, Review of form-finding methods for tensegrity structures. *International Journal of Space Structures*, 18,209–223, 2011.

[15] M. Yamamoto, B.S. Gan, K. Fujita, J. Kurokawa, A genetic algorithm based form-finding for tensegrity structure. *Procedia Engineering*, 14,2949–2956, 2011.

[16] R.E. Skelton, M. de Oliveira, Optimal complexity of deployable compressive structures. *Journal of The Franklin Institute*, 347,228–256, 2010.

[17] R.E. Skelton, M. de Oliveira, Optimal tensegrity structures in bending: the discrete Michell truss. *Journal of The Franklin Institute*, 347,257–283, 2010.

[18] R.E. Skelton, M. de Oliveira, *Tensegrity Systems*. Springer, 2010.

[19] K. Nagase, R.E. Skelton, Minimal mass tensegrity structures. *Journal of the International Association for Shell and Spatial Structures*, 55(1), 37–48, 2014.

[20] F. Fraternali, A. Marino, T. El Sayed, A. Della Cioppa, On the Structural Shape Optimization through Variational Methods and Evolutionary Algorithms. *Mechanics of Advanced Materials and Structures*, 18,224–243, 2011.

[21] N. Bel Hadj Ali, L. Rhode-Barbarigos, A.A. Pascual Albi, I.F.C. Smith, Design optimization and dynamic analysis of a tensegrity-based footbridge. *Engineering Structures*, 32(11),3650–3659, 2010.

[22] M.C. Phocas, O. Kontovourkis, M. Matheou, Kinetic hybrid structure development and simulation. *International Journal of Architectural Computing*, 10(1), 67–86, 2012.

[23] W.F. Baker, L.L. Beghini, A. Mazurek, L. Carrion, A. Beghini, Maxwell's reciprocal diagrams and discrete Michell frames. *Structural and Multidisciplinary Optimization*, Online first, DOI 10.1007/s00158-013-0910-0, 2013.

[24] R.E. Skelton, K. Nagase, Tensile tensegrity structures. *International Journal of Space Structures*, 27,131–137, 2012.

[25] R.E. Skelton, F. Fraternali, G. Carpentieri, A. Micheletti, Minimum mass design of tensegrity bridges with parametric architecture and multiscale complexity. *Mechanics Research Communications*, 58, 124–132, ISSN 0093-6413, doi: 10.1016/j.mechrescom.2013.10.017, 2014.

[26] R.E. Skelton, Structural systems: a marriage of structural engineering and system science. *Journal of Structural Controll*, 9,113–133, 2002.

[27] A.G.M. Michell, The limits of economy of material in frame-structures. *Philosophical Magazine*, 8,589–597, 1904.

[28] G. Bouchittè, W. Gangbo, P. Seppecher, Michell trusses and lines of principal action, *Mathematical Models & Methods In Applied Sciences*, 18,1571–1603, 2008.

[29] S. Dalil Safaei, A. Eriksson, A., G. Tibert, Optimum pre-stress design for frequency requirement of tensegrity structures. *Blucher Mechanical Engineering Proceedings* 1(1), 1258–1270, 2014.